 https://doi.org/10.1051/e3sconf/202338203004

Comparing the trend of V_s at similar range of saturated and unsaturated stress state variables.

Zhuoyuan Cheng[1*] and *Eng Choon* Leong[2]

[1]Singapore University of Social Sciences, School of Science and Technology, Singapore
[2]Nanyang Technological University, School of Civil & Environmental Engineering, Singapore

Abstract. The effect of matric suction on S-wave velocity (V_s) of unsaturated soils has been observed to show different trends from the V_s relationship with effective confining pressure. In some soils, the increase in S-wave velocity per unit stress change in matric suction (u_a-u_w) is greater than the increase in S-wave velocity per unit stress change in effective confining pressure (σ'_3) for saturated and dry soils and vice versa for other soils. In this study, the difference was examined through the stress state variables for unsaturated soils on similar soil samples. Experiments were conducted on sand and kaolin specimens using a triaxial cell modified to include bender elements and a high-air-entry disk for the testing of unsaturated soils. The soil specimens were first fully saturated and V_s at various effective confining pressures were measured. The tests were repeated with similar soil specimens subjected to net confining pressure and matric suction for similar stress range as the previous tests. Data was also collated from the literature. Comparisons were made by plotting on two-dimensional and three-dimensional plots to understand the differences. It was found that soil type and soil fabric play important role in the differences. Soil fabric plays a more important role for compacted soils where soil fabric is affected by the compaction water content.

1 Introduction

The variation of shear wave velocity (V_s) with effective confining pressure (σ'_3) [1-3], and matric suction (u_a-u_w) [3-7] has been investigated. The effects of both net confining stress (σ_3-u_a) and matric suction (u_a-u_w) on V_s has also been examined [8-11]. The findings show that V_s: (i) increases as effective confining pressure increases, and (ii) increases as the void ratio decreases with increasing matric suction or decreasing degree of saturation. However, no literatures examined the interaction of both saturated and unsaturated stress-state variables on the V_s of soils. According to [12], small-strain shear modulus (G_0) consists of two parts: one part ($G_{0,sat}$) is given by the net confining pressure (equal to effective confining pressure in the case of a saturated soil test) and the other part [$f(u_a-u_w)$] is given by the matric suction as shown in Equation (1).

$$G_o = G_{o,sat} + f(u_a - u_w) \tag{1}$$

From elastic wave theory, G_0 and V_s is related via Equation (2).

$$V_s = \sqrt{G_o/\rho} \tag{2}$$

where ρ is the bulk density of the soil.

The effect of an all-round net confining pressure acts on a soil may be different from that due to matric suction. If matric suction acts isotropically then the change in V_s per unit change of matric suction should be the same as the change in V_s per unit change of net confining pressure (σ_3-u_a). At low matric suction, [8] found that the change in G_o from variation in matric suction is equivalent to the variation in mean effective confining pressure. However, it is not clear how higher matric suction will affect G_o and hence, V_s.

In this study, the variation of Vs with effective confining pressure of saturated soils was used as a reference to examine the variation of V_s with matric suction of unsaturated soils. Bender element tests were conducted on fully saturated soil specimens at various effective confining pressures. The tests were repeated on similar soil specimens subjected to net confining pressure and matric suction. The matric suction and net normal stress values chosen in the tests have similar stress range as the effective confining stress in the tests on the saturated soil specimen. Data from literature were also collated and analysed together with test results from this study.

2 Materials and method

2.1 Materials

A coarse-grained soil and a fine-grained soil were selected for this study. Bender element tests were conducted using reconstituted specimens of river sand and kaolin. The properties of the soils and the test

* Corresponding author: zycheng@suss.edu.sg

conditions are summarized in Tables 1 and 2, respectively.

The specimen tag was separated into three parts. The first part represents the soil name. River sand specimens were labelled with "RS" and kaolin specimens were labelled with "KL". The second part represents the test condition. Saturated specimens were labelled with a "S" and unsaturated specimens were labelled with a "US". The last part represents the effective or net confining pressure applied to the specimens, e.g., 100 represents 100 kPa. All specimens have diameter of 50 mm and a height to diameter ratio of 1 to obtain clear wave signals.

Table 1. Properties of soils used for testing

Description	USCS/ Composition	Properties
River Sand (RS)	SM 70% Sand 30% Fines	$G_s = 2.65$ $C_u = 4.67$ $C_c = 0.21$
Kaolin (KL)	MH 100% Fines	$G_s = 2.65$ LL = 60 PL = 40

Table 2. Summary of test conditions

Specimen tag	Initial void ratio, e_0	Stress-state variables (kPa)		
		$(u_a\text{-}u_w)$	$(\sigma_3\text{-}u_a)$	$(\sigma_3\text{-}u_w)$
RS-US_100	0.51	0 - 38	100	-
RS-US_200	0.47	0 - 38	200	-
RS-US_400	0.51	0 - 38	400	-
RS-S	0.50	-	-	30 - 430
KL-US_200	1.66	0 - 400	200	-
KL-S	1.66	-	-	200 - 600

2.2 Experimental set-up and test procedures

The river sand was mixed with a predetermined amount of water (w = 15%) and compacted to an average void of about 0.475 via moist tamping procedures in a cylindrical split mould. The variation of void ratios of the compacted sand specimens were from 0.45 to 0.50. The specimens were then removed from the split mould and frozen so that rectangular slots could be etched out on both flat ends of the specimen to house the bender elements. The frozen sand specimens also reduced the difficulty of setting up the specimen in the triaxial cell.

The kaolin was prepared by consolidating kaolin slurry at an initial water content of 230% in a consolidation tank under a vertical load of 100 kPa. When consolidation was completed, the kaolin sample was extruded from the consolidation tank and trimmed to the specimens of dimensions 50 mm diameter and 50 mm height.

A modified triaxial apparatus (Fig. 1) was used in this study. The top cap was fitted with a porous disk while the bottom platen was fitted with a high air-entry ceramic disk. The air-entry value of the ceramic disk was 500 kPa. A bender element was fixed into each of the platen. Details of the modified triaxial apparatus has been reported in [13] and are not repeated here.

Once the specimen was set up in the triaxial cell, confining pressure and back pressure were applied. For the frozen sand specimen, an effective confining pressure of 30 kPa was applied initially and the specimen was left in the triaxial cell for one day to thaw. To ensure full saturation of the sand specimen, the effective confining pressure was reduced to 10 kPa and water was allowed to enter the specimen from the bottom platen using a GDS digital pressure-volume controller (DPVC). The top drainage line was connected to a vacuum pump to facilitate the removal of any entrapped air bubbles in the system. The procedures described above were repeated until the following conditions are met: (1) V_p remained constant [13]; (2) No air bubbles were observed in the top drainage line; and (3) Skempton's pore-pressure parameter B > 0.95 [14]. Upon saturation, the specimens were consolidated to the various stress conditions (Table 2). For unsaturated specimens, the top drainage line was connected to the air pressure system. Matric suction was imposed by applying air pressure (u_a) through the top drainage line via the top platen. The air pressure was held constant while the water pressure (u_w) at the bottom platen was reduced to establish the desired matric suction while maintaining the net confining pressure constant. Changes in the volume of water moving in and out of the specimen were monitored by the DPVC so that water content of the soil specimen at each stress condition can be calculated and the soil-water characteristics curve established (Fig. 2) using [15].

Bender element test was performed when the soil specimen was at equilibrium with the prescribed stress condition. The transmitting bender element was excited using a sinusoidal pulse. The compression (P) wave excitation frequency was 10, 20 and 50 kHz. The shear (S) wave excitation frequencies were 3, 5, 10 and 20 kHz. Signals were obtained at different excitation frequencies so that accurate arrival time could be obtained by comparing the recorded signals. Time-domain method was used to determine the arrival time. Arrival time for the P-wave signals was determined from the first deflection in the receiver signal. Arrival time for the S-wave was determined from the zero after first bump in the receiver signal [16-18]

Testing under saturated and unsaturated conditions using similar pressure range enabled the S-wave velocities to be compared when the soil specimen was subjected to an effective confining pressure when the oil specimen was saturated and a combination of net confining pressure and matric suction.

3 Results and Discussions

If the effect of matric suction is the same as net confining pressure, plotting V_s against the sum of net confining pressure and matric suction $[(\sigma_3\text{-}u_a)+(u_a\text{-}u_w)]$ should show a similar plot as V_s plotted against σ'_3 as shown in Fig. 3 and 4 for river sand and kaolin, respectively.

Fig. 3 shows that the effect of $(u_a\text{-}u_w)$ on V_s for river sand is more than the effect of σ'_3 on V_s for the saturated sand specimen. As $(\sigma_3\text{-}u_a)$ increases, the effect of $(u_a\text{-}u_w)$ on V_s decreases till it is almost the same as effect of σ'_3 on V_s. For the kaolin specimen, the increase in $(u_a\text{-}u_w)$

 https://doi.org/10.1051/e3sconf/202338203004

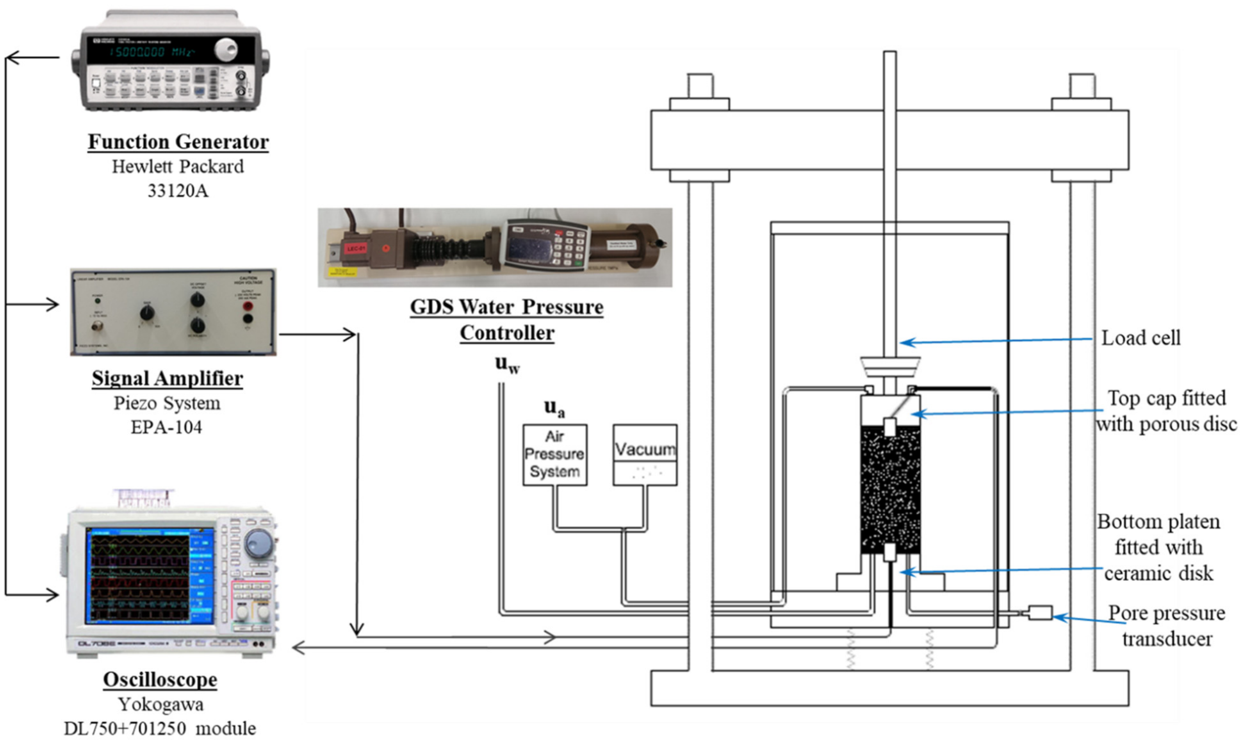

Fig. 1. Modified triaxial set-up

has the same effect as the increase in σ'_3 on V_s as shown in Fig. 4. This difference in trend of the V_s with increase in (u_a-u_w) was further explored using data from other researchers plotted in similar way as shown in Figs. 5 - 7. The properties of the soils tested by other researchers are tabulated in Table 3.

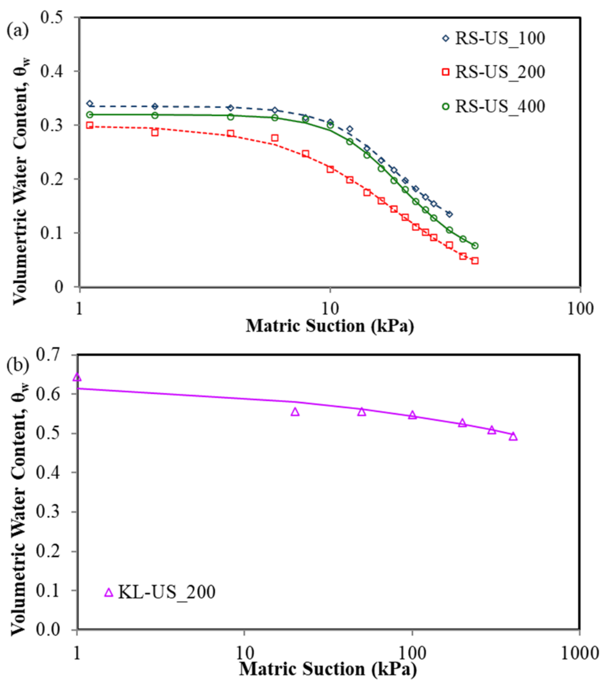

Fig. 2. Soil water characteristic curve of (a) River sand and (b) kaolin specimens.

Resonant column tests were conducted on loose sand at (σ_3-u_a) of 6.9, 17.25 and 34.5 kPa for [9]. The specimens were subjected to matric suctions of 6.9 to 110 kPa. Results were presented in term of G_o with matric suction at different net normal stresses. A constant bulk density of 1700 kg/m^3 was assumed based on [19] to convert the G_o to V_s using Equation (2). The (u_a-u_w) was shown to contribute lesser to the increase in V_s compared to σ'_3 for the loose sand [9]. The different trend in V_s observed for the loose sand from [9] and River sand in this study is likely due to the River sand being better graded with a higher percentage of non-plastic fines compared to the loose sand from [9]. This lowers the void ratio and creates smaller pore radius in River sand which results in greater surface tension between the soil particles. The resulting (u_a-u_w) acts to "pull" the particles closer to create a stiffer specimen resulting in a more than proportional increase in V_s. This indirectly explains the less than proportional contribution of (u_a-u_w) to V_s for the loose sand from [9].

The V_s data from [10] and [11] were obtained for soils with a high percentage of silt and clay. The shear wave velocities of recompacted completely decomposed tuff (CDT) under both saturated and unsaturated conditions were measured to investigate the degree of stiffness anisotropy [10]. The V_s for the saturated soil specimen shows non-linear increase with σ'_3 that can be best fitted with a power function (Fig. 6). Plotting V_s of the unsaturated specimens against [(σ_3-u_a)+(u_a-u_w)] shows the V_s lies close to the best-fit line of the V_s of the saturated specimen indicating that the effects of σ'_3 and (u_a-u_w) on V_s are similar

The V_s of a compacted clayey sand were measured in a suction-controlled triaxial apparatus using bender elements [11]. Like [10], V_s for the saturated soil specimen shows non-linear increase with σ'_3 that can be described using a power function (Fig. 7). Plotting V_s of the unsaturated specimens against [(σ_3-u_a)+(u_a-u_w)] shows the V_s deviates from and lies above the power-law curve of the saturated V_s. Hence, the contribution of

(u_a-u_w)] to V_s is slightly greater than the contribution of σ'_3 to V_s.

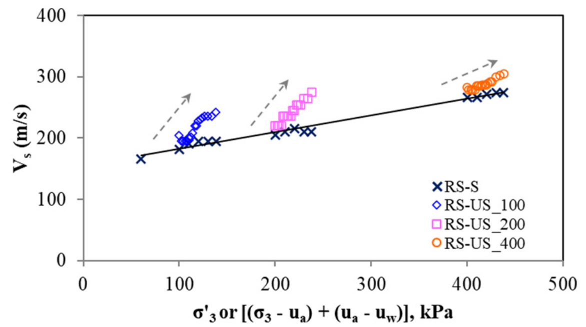

Fig. 3. Effect of effective confining pressure and combined net confining pressure and matric suction on V_s for River sand specimens.

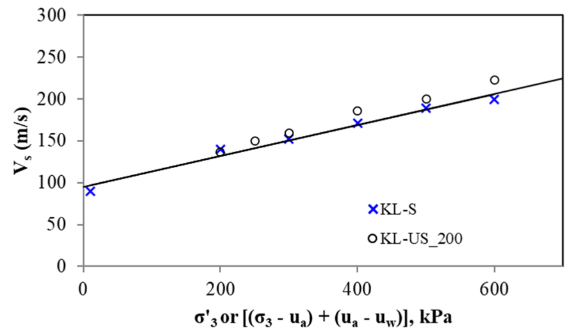

Fig. 4. Effect of effective confining pressure and combined net confining pressure and matric suction on V_s for kaolin specimens.

Table 3. Properties of soils from literature

Description	USCS/ Composition	Properties
Loose sand [9]Hoyos et al. (2008)	SP/ 98% Sand 2% Silt	$G_s = 2.65$ $C_u = 1.78$ $C_c = 0.82$
Completely decomposed tuff [10] Ng and Yung (2008)	ML/ 24% Sand 72% Silt 4% Clay	$G_s = 2.73$ $C_u = 4.55$ $C_c = 0.61$ LL = 43 PL = 29
Clayey sand [11]Georgetti et al. (2013)	SC/ 67% Sand 5% Silt 28% Clay	LL=32 PL=16

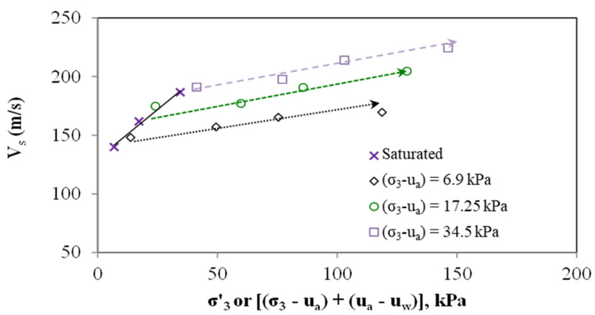

Fig. 5. Effect of subjected stress on V_s for loose sand (data from [9])

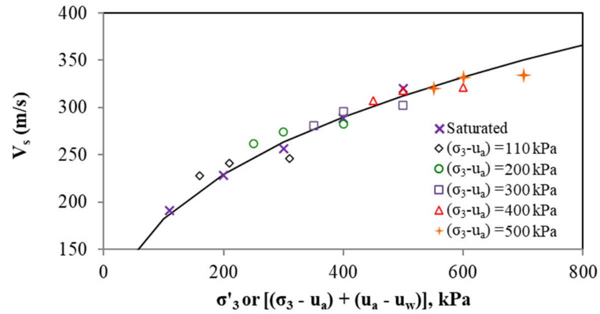

Fig. 6. Effect of effective confining pressure and combined net confining pressure and matric suction on V_s for completely decomposed tuff specimens (data from [10])

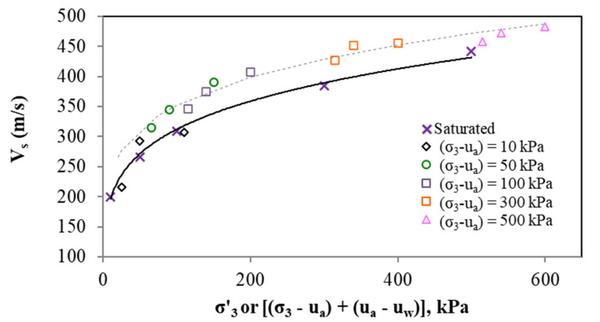

Fig. 7. Effect of effective confining pressure and combined net confining pressure and matric suction on V_s for clayey sand specimens (data from [11])

The differences in trend show the effect of stress anisotropy on V_s for unsaturated soils. To better understand the interaction between the stress-state variables, the data are replotted as 3D-plots in Figs. 8 to 12. According to [20-22], G_o is proportional to the $\sqrt{(\sigma'_3)}$. Therefore, according to Equation (2), V_s is proportional to $(\sigma'_3)^{0.25}$. The relation of (u_a-u_w) for G_o or V_s is not well studied. From the above discussions, it can be expected that the contribution of (u_a-u_w) to V_s will also assume a similar form as that for σ'_3. On account of Figures 3 to 7, it can also be postulated that the increase in V_s from (u_a-u_w) is dependent on (σ_3-u_a). Hence from Equation 1, a similar equation for V_s can be postulated for unsaturated soils as given by Equation 3.

$$V_s = C_1\left(\frac{\sigma_3 - u_a}{p_a}\right)^{0.25} + C_2\left(\frac{u_a - u_w}{\sigma_3 - u_a}\right)^{n} \qquad (3)$$

where C_1, C_2 and n are constants depending on the soil, and p_a is atmospheric pressure (≈100 kPa) used to normalise (σ_3-u_a) such that C_1 and C_2 has the same units as V_s. The constant n has no units.

The data in Figs. 8 to 12 are hence plotted with $[(u_a-u_w)/(\sigma-u_a)]^n$ and $[(\sigma'_3-u_a)/p_a]^{0.25}$ as the x- and y-axes, respectively. The value of n is indicated in the x-axis label of the respective figures. The data are fitted with a planar surface using MATLAB via a polynomial equation (Equation 4) of first degree ("poly11"). The coefficients and R^2 of the fitted surfaces are tabulated in Table 4. All the data fall on or close to the fitted plane with R^2 above 0.9.

$$poly11(x, y) = p_{00} + p_{10}x + p_{01}y \quad (4)$$

where x = $[(u_a-u_w)/(\sigma-u_a)]^n$ and y = $(\sigma_3-u_a)^{0.25}$

The intercept p_{00} represents the V_s when both matric suction and net normal stress are not present. However, two soils (completely decomposed tuff from [10] and River sand) show negative values for p_{00}. For these cases, the negative values imply that V_s is zero or not measurable until either $(\sigma-u_a)$ or both $(\sigma-u_a)$ and (u_a-u_w) are present.

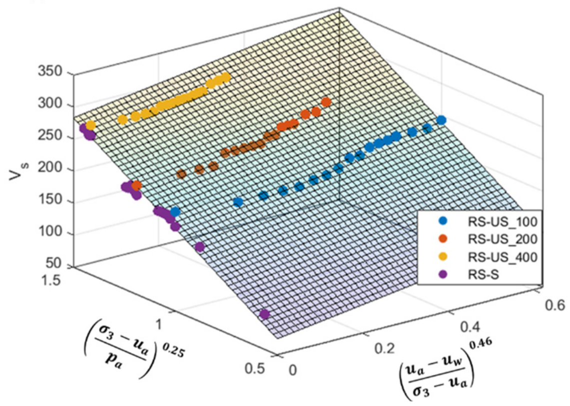

Fig. 8. Variation of V_s with net normal stress and matric suction for River sand specimens

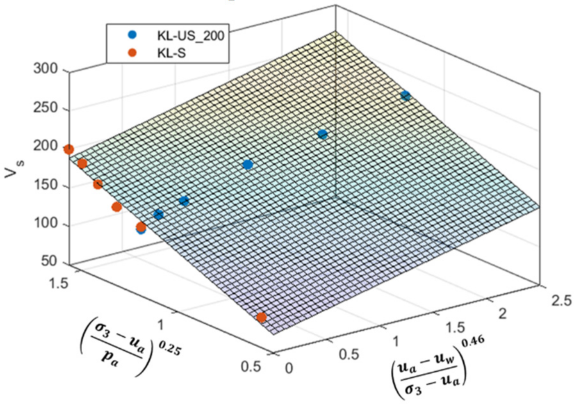

Fig. 9. Variation of V_s with net confining pressure and matric suction for kaolin specimens

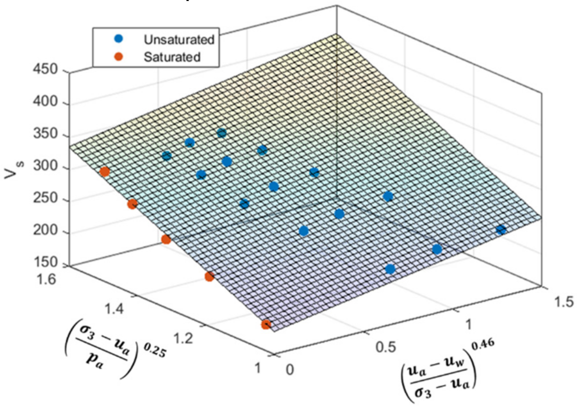

Fig. 10. Variation of V_s with net confining pressure and matric suction for loose sand (data from [9])

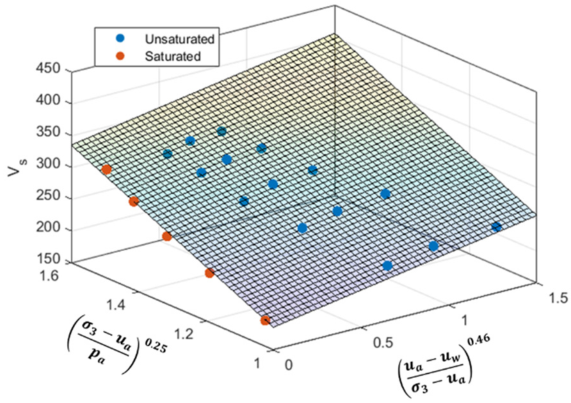

Fig. 11. Variation of V_s with net confining pressure and matric suction for completely decomposed tuff (data from [10])

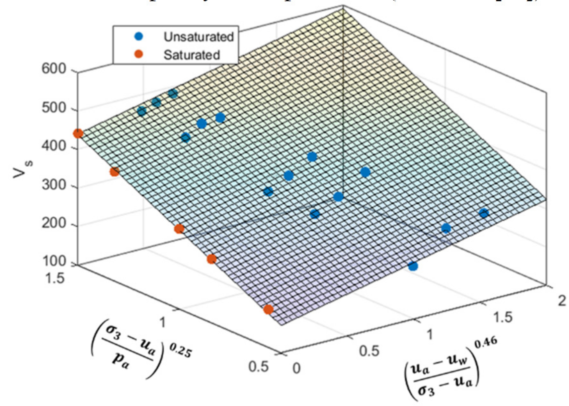

Fig. 12. Variation of V_s with net confining pressure and matric suction for clayey sand (data from [11])

Table 3. Parameters and R^2 of fitted surface

Description	P_{00}	P_{10}	P_{01}	R^2
[9]	15.66	14.73	228.1	0.927
[10]	-62.31	46.95	248.3	0.984
[11]	38.93	75.49	267	0.953
Kaolin	20.59	31.01	107	0.956
River sand	-28.09	97.45	207.3	0.955

4 Conclusion

In this study, V_s of two soils (River sand and kaolin) in saturated and unsaturated conditions were obtained using bender elements in a triaxial set-up. The tests were conducted on several similar specimens where the unsaturated specimens were subjected to similar stress ranges as the saturated specimens. The experimental results and data collated from literature were analysed to understand the differences in trend in the effect of matric suction on S-wave velocity (V_s) of unsaturated soils from the V_s relationship with effective confining pressure of saturated soils.

The variation of V_s with effective confining pressure for saturated soils and the variation of V_s with net confining pressure and matric suction were examined in 2D plots. The 2D plots show that the variation of V_s with net confining pressure and matric suction can be similar, below or above the variation of Vs with effective confining pressure of saturated soils.

It is postulated that V_s can be described in a similar fashion as small-strain shear modulus with one part given by the net confining pressure (or effective confining pressure for saturated soils) and another part given by the matric suction. The variation of V_s with net confining pressure can be described using a power law with exponent of 0.25. The variation of V_s with matric suction is dependent on the prevailing net confining pressure and is also a power law as well. But the exponent n is dependent on the soil.

The relationship of V_s with $[(u_a-u_w)/(\sigma-u_a)]^n$ and $[(\sigma_3-u_a)/p_a]^{0.25}$ as two independent axes is examined using a 3D plot. It was found that a plane can be used to fit both saturated and unsaturated V_s data. Further research will be carried out to investigate the relationship between the fitted coefficients of the plane and soil parameters to develop a model to estimate V_s for unsaturated soils under different stress conditions.

References

1. Hardin, B.O. & Richart, F.E.Jr., J. of the Soil Mechanics and Foundations Division, **89**, SM1, 33-65 (1963)
2. Santamarina, J.C., Klein, K.A., Fan, M.A., Soils and Waves (2001)
3. Whalley, W.R., Jenkins, M., & Attenborough, K., Soil Science Society of America J., **75**, 5, 1652-1657 (2011)
4. Alramahi, B., Alshibli, K.A., Fratta, D., & Trautwein, S., Geotechnical Testing J., **31**, 1, 12-23 (2008)
5. Suwal, L.P. & Kuwano, R., Soils and Foundations, **58**, 6, 1553-1562 (2018)
6. Ngoc, T.P., Fatahi, B. & Khabbaz, H., Int. J. Geomech. **19**, 8 (2019)
7. Mahmoodabadi, M. & Bryson, L.S., Int. J. of Geomechanics, **21**, 1 (2021)
8. Vinale, F., d'Onofrio, A., Mancuso, C., Santucci de Magistris, F. & Tatsuoka, F., *The pre-failure behavior of soils as construction materials*, in Proceedings of the 2nd Int. Symposium on Pre-failure Deformation Characteristics of Geomaterials, Torino, Italy, 955–1007 (1999)
9. Hoyos, L.R., Takkabutr, P., Puppala, A.J. & Hossain, Md.S., *Dynamic response of unsaturated soils using resonant column and bender element testing techniques*, in Proceedings of the Geotechnical Earthquake Engineering and Soil Dynamics IV, Sacramento, California, 1-8 (2008)
10. Ng, C.W.W. & Yung S.Y., Géotechnique, **58**, 1, 23–35 (2008)
11. Georgetti, G.B., Vilar, O.M. & Rodrigues, R.A., *Small-strain shear modulus and shear strength of an unsaturated clayey sand*, in Proceedings of the 18th Int. Conference on Soil Mechanics and Geotechnical Engineering (2013)
12. Leroueil, S. & Hight, D., *Behaviour and properties of natural soils and soft rocks*, in Characterisation and engineering properties of Natural Soils, Lisse, the Netherlands, **1**, 29 (2003)
13. Leong, E.C. & Cheng, Z.Y., Int. J. of Geomechanics, **16**, 6 (2016)
14. Head, K.H., Manual of Soil Laboratory Testing, Volume 3: Effective stress tests (1998)
15. Fredlund, D.G. & Xing, A., Canadian Geotechnical J., **31**, 4, 521-532 (1994)
16. Sanchez-Salinero, I., Roesset, J.M. & Stokoe, K.H., *Analytical Studies of Body Wave Propagation and Attenuation*, in Report GR 86-15, Civil Enginerring Department, University of Texas, Austin, United States (1986)
17. Arulnathan, R., Boulanger, R.W., Riemer, M.F., Geotechnical Testing J., **21**, 2, 120–131 (1998)
18. Leong, E.C., Cahyadi, J. and Rahardjo, H., Geotechnical Testing J., **28**, 5, 792–812, (2009).
19. Takkabutr P., *Experimental investigations on small strain stiffness properties of partially saturated soils via resonant column and bender element testing*, PhD thesis, University of Texas, Arlington (2006)
20. Hardin, B.O. and Black, W.L., J. of the Soil Mechanics and Foundations Division, **94**, SM2, pp. 353-369 (1968)
21. Hardin, B.O. and Drnevich, V.P., J. of Soil Mechanics & Foundations Division, **98**, 6, 603-624 (1972)
22. Hardin, B.O. and Drnevich, V.P., J. of the Soil Mechanics and Foundations Division, **98**, 7, 667-692 (1972)